

We are IntechOpen, the world's leading publisher of Open Access books Built by scientists, for scientists

4,800

Open access books available

122,000

International authors and editors

135M

Downloads

Our authors are among the

154

Countries delivered to

TOP 1%

most cited scientists

12.2%

Contributors from top 500 universities



WEB OF SCIENCE™

Selection of our books indexed in the Book Citation Index
in Web of Science™ Core Collection (BKCI)

Interested in publishing with us?
Contact book.department@intechopen.com

Numbers displayed above are based on latest data collected.

For more information visit www.intechopen.com



Wear Behaviour of Aluminium Alloy 8011 with 4% Fly Ash Composites by Using Sensitivity Analysis

Subramaniam Magibalan

Abstract

The current research work is focused on fabrication of Aluminium Alloy 8011 with 4% fly ash composite (AA8011-4% FA) by using the stir casting method. Wear behaviour and description of the composite are evaluated in different process parameters by using a pin-on-disc at room temperature. Fly ash (FA) in the range of (4 wt. %, average micron size 10–30 μm) is included into the matrix, and its sensitivity analysis is investigated. Three level of Central Composite Design model is developed by using Response Surface Methodology equation with different process parameters via load, time and sliding velocity are separate in the range of (5–15 N), (5–15 min) and (1.5–4.5 m/s) respectively. The surface plot shows that wear rate increases with increasing load, time and sliding velocity. A sensitivity analysis is also carried out and compared with the relative impact of input parameters on wear behaviour in order to verify the measurement errors on the values of the uncertainty in estimated parameters of three inputs such as normal load, time and sliding velocity on wear rate (WR) and coefficient of friction (COF). The result shows that normal load is more sensitive than the other parameters. The variation of load causes more changes in wear rate.

Keywords: aluminium alloy 8011 (AA8011), fly ash (FA), response surface methodology (RSM), wear rate (WR), coefficient of friction (COF), sensitivity analysis (SA)

1. Introduction

Metal matrix composites (MMCs) occur as an essential category of material used in space and transportation industries. There is an inclusive in dropping the wear in demand to decrease the tradition of material properties and expenditure of energy. This controlling of wear should be considered cautiously from the idea of choosing the alloy composition, reinforcement and additionally the process techniques. The incorporation of hard reinforcement segments, particulates, fibres and whiskers has been capable of these composites through smart tribological characteristics [2, 8, 12–18].

These reinforcements will either be value-added ex-situ or created as in-situ composites within the dissolved. It is glowing well-known that in-situ supports stay

of the many smart benefits appreciate wholesome boundary and extraordinary affection power through the medium, homogeneously circulated minor parts within the matrix, extraordinary mechanical assets and low cost. In-situ ceramic mixtures appreciate Al_2O_3 [23], TiB_2 [1] and TiC [24] widely occupied as reinforcements in aluminium fabricated composites.

Aluminium ash composites can be synthesised through the liquid metal stir casting, compo casting (semi-solid processing), changed compo casting and squeeze casting techniques. The stir casting route product is well distributed, moderately agglomerate and consistent free fly ash particle composites [1–4].

AA2011 matrix reinforced with SiC reinforcement (5 & 10%) produced by liquid metallurgy route. SiC abrasive wear rate is increased with increasing applied load, sliding distance and element size compared for Al_2O_3 emery paper is used means the wear rate increase of element size, applied load decrease with increasing the sliding distance and at the same time, the abrasive size was more effective for both matrix and composite [5].

AA6061 with 1% of CNT reinforcement is produced by ball milling and spark plasma process and it is reported that the mild wear rate and friction coefficient are low compared to the monolithic 6061 alloy [6].

The wear rate in a concession of weight loss per unit sliding distance, coefficient of friction and volume loss continues to achieve for the metal matrix composites. The results of the composite show higher wear resistance than matrix metal [7].

AA7075/graphite composite materials with (5–20) wt.% are fabricated by a liquid casting technique and pin on disc method to calculate the wear rate. The coefficient of friction is compact with the calculation of graphite content and stretched a minimum at 5 wt. % graphite content [8].

Develops the mathematical typical is settled by mistreatment regression analysis methodology for the expectation of damage performance of the MMC besides sufficiency of the prototypical has been valid expending analysis of variance (ANOVA) methods. Finally, the inflation of parameter has in addition been done using style trained software package. The results ensure unprotected that response surface methodology (RSM) may be a smart tool for expectation of wear behaviour below combined sliding and rolling action [9].

Develops a regression prototypical is valid by normal mathematics code SYSTAT 12 and normal arithmetic tools equivalent to analysis of variance (ANOVA) and student's t-check. It has been found that establishing the regression prototypical is also effectively wished to calculate the wear rate at 95% confidence level and expected trends are mentioned with the assistance of worn surface morphologies. The results of the composite show higher wear of the metal matrix [10].

Develops a mathematical model to predict the wear rate of AA6061/ (0–10%) ZrB_2 in-situ composites. The factors thought of area unit sliding speed, sliding distance, traditional load and mass fraction of ZrB_2 particles. The impact of those factors on the damage proportion of the made-up composite is examined and additionally, the expected trends are mentioned by perceptive the injury surface morphologies [11].

Sensitivity analysis of the process parameters of gas metal arc welding process of welding speed, voltage and current. Based on the result, we represent the success of the processing parameters and showed that the change of process parameters influences the bead width and bead height with further strong penetration [19].

The effect of welding on flux cored arc welding material of 317 L on a structural steel plate. The process parameters used in the experiment were welding current, speed and nozzle to plate distance. Sensitivity analysis has been applied to find out the process parameters with the most influence on the bead geometry. Sensitivity

analysis shows that bead width, dilution, area of penetration and coefficient of internal shape are mostly affected by the change of process parameters [20].

We investigated the sensitivity analysis of weld bead parameters such as bead width, bead height and penetration to variations in current, voltage and speed in the submerged arc welding process. The result shows that bead width is more sensitive to voltage and speed variations than bead height and penetration [21].

Sensitivity analysis to predict the tensile strength of friction stir welded alloy AA7039 aluminium. Based on the result they concluded, it was found that the sensitivities of rotational speed cause large changes in tensile strength when the RPM increases compared with welding RPM and axial force [22].

In the present work, an attempt is made to develop a mathematical model to calculate the wear rate of (AA8011-4% FA) composite and analyse the impact of normal load (N), time (min) and sliding velocity (m/sec) on wear rate and coefficient of friction. Interestingly, mathematical models are conducted consistent with central composite rotatable utilised. Mathematical models are established to predict the impact of method constraints on the responses. Finally, the sensitivity results are compared and verified with the experimental result.

2. Dry sliding wear test

The tribological properties of the samples were assessed using a dry sliding wear test for different number of specimens by using a pin-on-disc machine as shown in **Table 1**.

Figure 1 reveals that the surface of each pin and disc is clean with a soft paper soaked in resolving before actual testing. The fabric loss from the composite surface is measured employing exactness electronic balancing machine with an accuracy of ± 0.0001 g. Wear rate is unique of the maximum significant criteria on behalf of formative the pin-on-disc operation. Higher wear rate is always preferred in such operations. Wear rate was measured from the weight loss. Each trial was repeated twice and the average weight loss was taken for the analysis of wear rate. In this study, the machining performance and the mathematical model were evaluated

S.No.	Description	Details
1.	Make & Model	DUCOM, TR-20LE-PHM-400
2.	Normal load range	5–15 N
3.	Disc speed	100–1000 rpm
4.	Pre-set timer range	5–15 min
5.	Wear disc thickness	8 mm (EN 31 steel (C, 1.00%; Si, 0.20%; Mn, 0.50%; Cr, 1.40%; hardness of 60 HRC)
6.	Wear disc track diameter	90 mm
7.	Specimen pin diameter	10 mm
8.	Pin length	50 mm
9.	ASTM standard	G99
10.	Measurement and real-time data acquisition	Wear, friction, COF and temperature.

Table 1.
Specification of wear testing equipment.

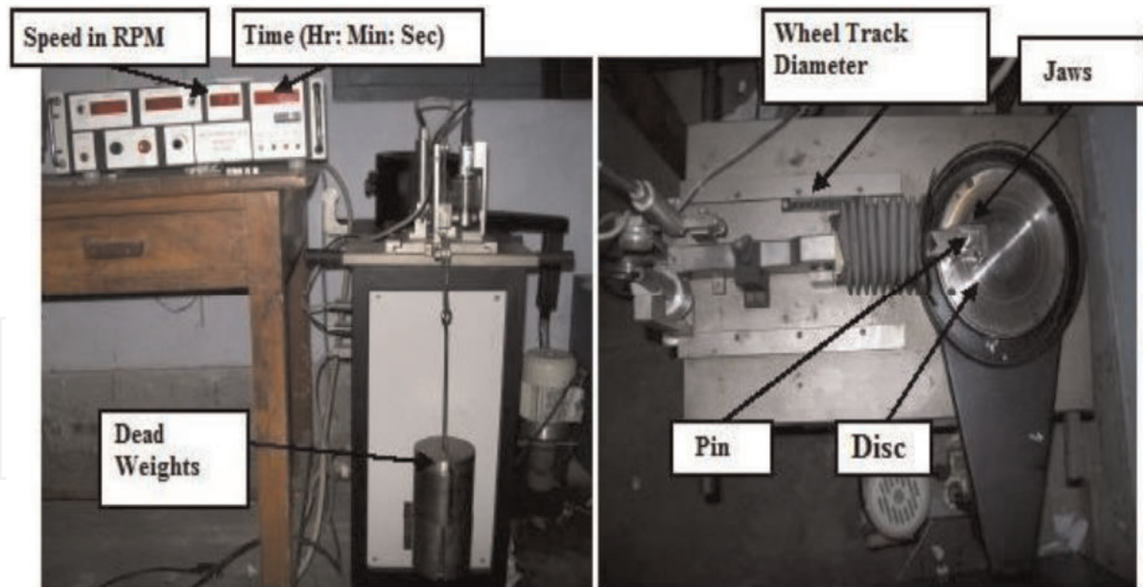


Figure 1.
Pin-on-disc wear experimental setup.

using Eqs. (1) and (2). **Tables 2 and 3** show that the setup of the experiment was designed on the idea of the central composite design (CCD) technique.

$$Wear\ rate\ (g/\ min) = \frac{\text{metal removed (part)}}{\text{(Time of machining)}} \quad (1)$$

The factorial portion of CCD is a full factorial design with all mixtures of the factors at three levels (+1, 0, -1) and composed of the eight-star points and six central points (coded level 0), which were the centre between the high and the low levels. The star points were at the face-centre of the cube portion that corresponds to an α value of 1 and this sort of design was usually known as the “face-centred CCD.” The tests were conducted using stipulated conditions in keeping with the face-centred CCD with 20 experimental observations at three independent input variables [15–18].

$$Y_u = b_0 + \sum_{i=1}^k b_i x_i + \sum_{i=1}^k b_{ii} x_i^2 + \sum_{j>1}^k b_{ij} x_i x_j \quad (2)$$

Y_U is the response.

x_i (1, 2 ... k) is the coded levels of k numerical variables.

b_0 —endless term.

b_i —linear term.

b_{ii} —quadratic term.

b_{ij} —interaction term.

Parameter	-1	0	1
Load (N)	5	10	15
Time (min)	5	10	15
Sliding velocity(m/sec)	1.5	3	4.5

Table 2.
Process parameters and their levels.

Run	Load (N)	Time (min)	Sliding velocity (m/sec)	WR (g/min) $\times 10^{-5}$	COF (μ) $\times 10^{-2}$
1	5	5	1.5	342	55.9
2	15	5	1.5	434	37.2
3	5	15	1.5	372	49.7
4	15	15	1.5	484	54.2
5	5	5	4.5	428	36.9
6	15	5	4.5	534	33.4
7	5	15	4.5	454	26.6
8	15	15	4.5	585	45.2
9	5	10	3.0	422	52.3
10	15	10	3.0	535	52.3
11	10	5	3.0	398	34.4
12	10	15	3.0	434	37.5
13	10	10	1.5	380	38.3
14	10	10	4.5	466	24.9
15	10	10	3.0	430	38.2
16	10	10	3.0	435	38.0
17	10	10	3.0	434	38.4
18	10	10	3.0	430	38.6
19	10	10	3.0	432	38.4
20	10	10	3.0	432	38.2

Table 3.
Design of experiment matrix and wear characteristics.

2.1 Design of experiment

In this study, a second-order polynomial was selected to develop empirical equations to represent responses (wear rate and COF) in terms of controllable variables such as normal load (A), time (B) and sliding velocity (C). The final response equations were developed for wear rate and COF using the experimental results.

This mathematical prototypical has been achieved to reproduce the independent, quadratic and interactive effects of some machining parameters on the machined for wear rate (WR) and coefficient of friction (COF). The empirical relationship for correlating the WR and COF the thought of dry sliding wear method parameters is obtained as follows:

$$\begin{aligned} \text{WR (g/min)} \times 10^{-5} = & 317.31 - 30.17 A + 14.41 B + 48.85 C + 1.8673 A^2 \\ & - 0.6327 B^2 - 3.919 C^3 + 0.2250 A \times B + 0.550 A \times C \\ & - 0.050 B \times C \end{aligned} \quad (3)$$

$$\begin{aligned} \text{COF } (\mu) \times 10^{-2} = & 97.512 - 14.661 A + 0.639 B + 10.816 C + 0.54745 A^2 \\ & - 0.10655 B^2 - 3.1172 C^2 + 0.22650 A \times B + 0.4883 A \times C \\ & - 0.1550 B \times C \end{aligned} \quad (4)$$

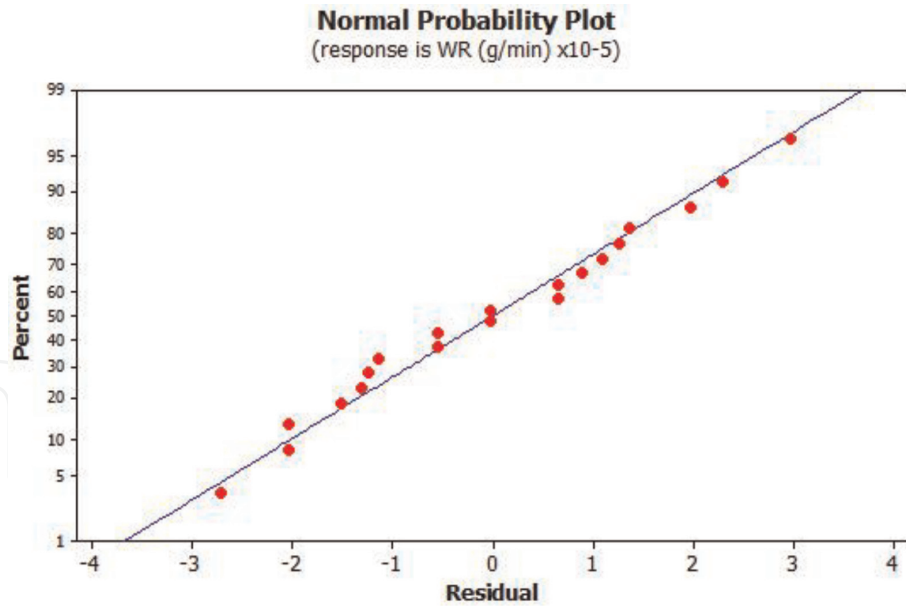


Figure 2.
Standard probability plot for wear rate.

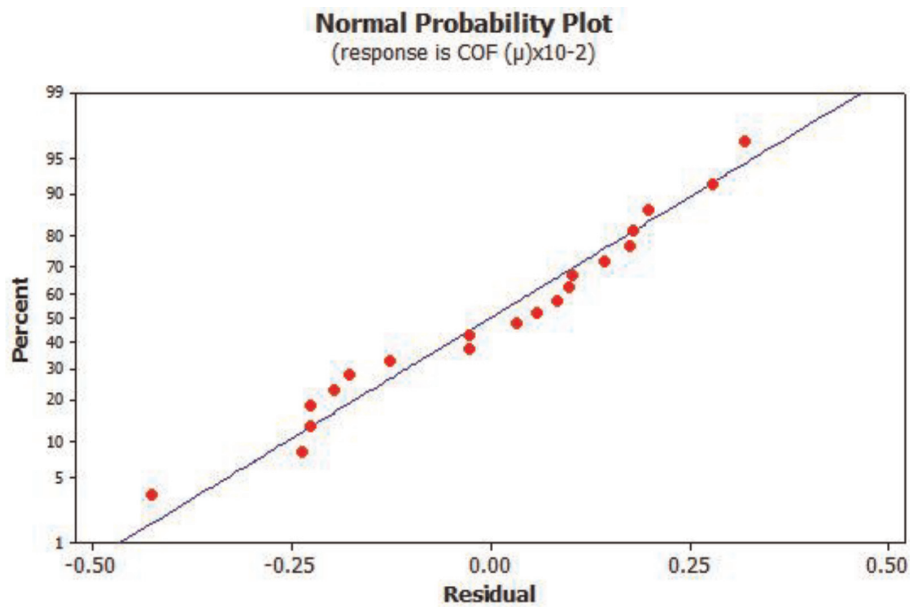


Figure 3.
Standard probability plot for COF.

Source	DF	Adj SS	Adj MS	F-value	P-value
Model	9	61981.7	6886.86	1458.03	0.000
Linear	3	3875.2	1291.72	273.47	0.000
Square	3	6472.3	2157.45	456.76	0.000
2-Way interaction	3	390.4	130.12	27.55	0.000
Error	10	47.2	4.72		
Lack-of-fit	5	26.4	5.28	1.27	0.401
Pure error	5	20.8	4.17		
Total	19	62029.0		$R^2 = 99.92\%$	

Table 4.
Analysis of variance table for wear rate.

Source	DF	Adj SS	Adj MS	F-value	P-value
Model	9	1400.34	15.559	2051.03	0.000
Linear	3	490.29	163.429	2154.31	0.000
Square	3	535.42	178.475	2352.64	0.000
2-Way interaction	3	374.63	124.878	1646.13	0.000
Error	10	0.76	0.076		
Lack-of-fit	5	0.54	0.108	2.45	0.174
Pure error	5	0.22	0.044		
Total	19	1401.10		R ² = 99.95%	

Table 5.
 Analysis of variance table for COF.

Eq. (3) and (4) develop empirical models based on the composite desirability optimisation technique. **Figures 2** and **3** show that the experimental values and predicted values from the mathematical model are scattered on both sides and close to 45° line, which further proves the adequacy of the model.

The normal percentage point of F-ratio dispersal for 95% confidence limit is 5.05 as shown in **Tables 4** and **5**. The F -values (1.27 and 2.45) aimed at deficiency of adequate are lesser than the normal value. Thus WR and COF the prototypically stand adequate.

3. Sensitivity analysis

After eliminating the non-significant terms in Eq. (3) and (4), the final response equations for wear rate and coefficient of friction are given below.

$$\begin{aligned} \text{WR (g/min)} \times 10^{-5} = & 317.31 - 30.17 A + 14.41 B + 48.85 C + 1.8673 A^2 \\ & - 0.6327 B^2 - 3.919 C^2 + 0.2250 A \times B + 0.550 A \times C \end{aligned} \quad (5)$$

$$\begin{aligned} \text{COF } (\mu) \times 10^{-2} = & 97.512 - 14.661 A + 0.639 B + 10.816 C + 0.54745 A^2 \\ & - 0.10655 B^2 - 3.1172 C^2 + 0.22650 A \times B + 0.4883 A \times C \\ & - 0.1550 B \times C \end{aligned} \quad (6)$$

From the developed mathematical Eqs. (5) and (6) to be used for the estimation of wear rate and coefficient of friction, the sensitivity equations are obtained by differentiating Eqs. (5) and (6) with respect to process parameters of load (A), time (B), and sliding velocity (C) as given below.

$$\frac{d\text{WR}}{dA} = -30.17 + 1.8673 * 2A + 0.2250 B + 0.550 C \quad (7)$$

$$\frac{d\text{COF}}{dA} = -14.661 + 0.5475 * 2A + 0.2265 B + 0.4883 C \quad (8)$$

$$\frac{d\text{WR}}{dB} = 14.41 - 0.6327 * 2 B + 0.2250 A \quad (9)$$

$$\frac{d\text{COF}}{dB} = 0.639 - 0.1065 * 2 B + 0.2265 A - 0.1550 C \quad (10)$$

$$\frac{dWR}{dC} = 48.85 - 3.919 * 2 C + 0.550 A \quad (11)$$

$$\frac{dCOF}{dC} = 10.816 - 3.1172 * 2 C + 0.4883 A - 0.1550 B \quad (12)$$

Results of WR and COF for sensitivities of load, time, sliding velocity on WR and COF are presented in **Tables 6** and **7**.

Load (N)	B = 10 min, C = 3 m/sec		
	$\frac{dWR}{dA}$	$\frac{dWR}{dB}$	$\frac{dWR}{dC}$
5	-34.6796	15.4504	56.1380
10	-30.1700	14.4100	48.8500
15	-25.6604	13.3696	41.5620

Table 6.
Wear rate for sensitivities of process parameters.

Load (N)	B = 10 min, C = 3 m/sec		
	$\frac{dCOF}{dA}$	$\frac{dCOF}{dB}$	$\frac{dCOF}{dC}$
5	-16.4708	0.7805	16.7171
10	-14.6610	0.6390	10.8160
15	-12.8512	0.4975	4.9149

Table 7.
COF for sensitivities of process parameters.

4. Results and discussion

4.1 Effects of load and time on wear rate

The influence of response surface plot for wear rate is shown in **Figure 4**. Wear rate increases with the increase of applied load, but the time also increases when wear rate increases. The frictional heat can result in excessive deterioration of the composite transfer from materials to the disc counterpart. The increase of applied load inspiration to disproportionate damage of the composite and thus results shows an increase in wear rate.

4.2 Effect of time and sliding velocity on COF

In **Figure 5** shows that the impression residues, the disc considerable develops worn and guarded material derives currently contact with the pin, scratching of the disc shallow origins the ploughing and later friction coefficient increase with a period of impression. After the period of impression the expansion of irregularity and alternative constraints might influence a particular solid value. Therefore, the standards of friction coefficient endure endless for the repose. This can be described by the mechanism that with the wear occurrence below process, supplementary fly ash particles are made with the effect of sliding velocity, consequently, the being of the fly ash disturbs at the connected area and intersection asset and so subsidises directly to the complex level of friction coefficient.

Surface Plot of WR (g/min) x10⁻⁵ vs Time (min), Load (N)

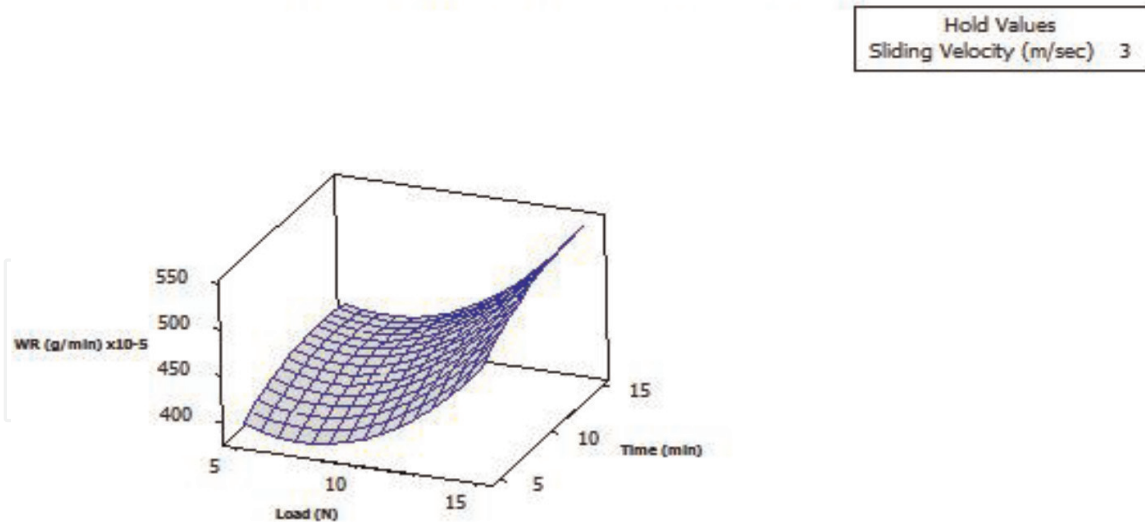


Figure 4.
Effects of load and time on the wear rate.

Surface Plot of COF (μ)x10⁻² vs Sliding Velocity (m/sec), Load (N)

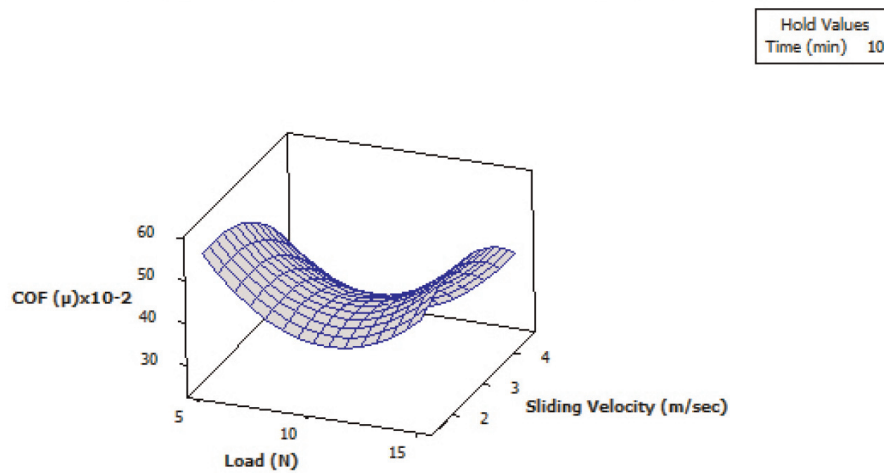


Figure 5.
Influence of time and sliding velocity on COF.

B=10 min, C=3 m/sec

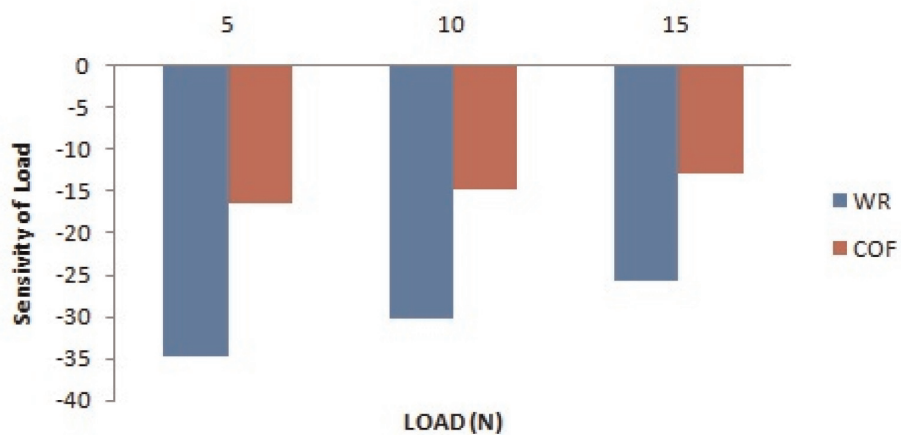


Figure 6.
Sensitivity analysis results of load.

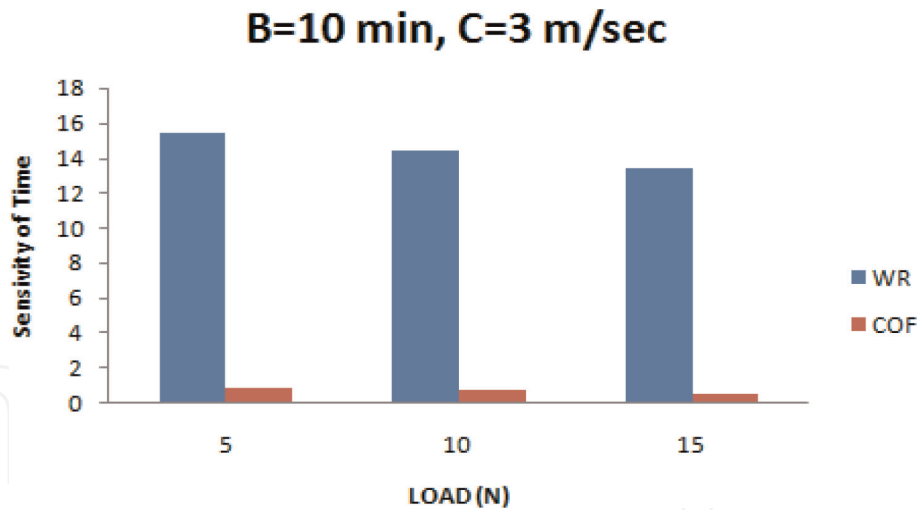


Figure 7.
Sensitivity analysis results of time.

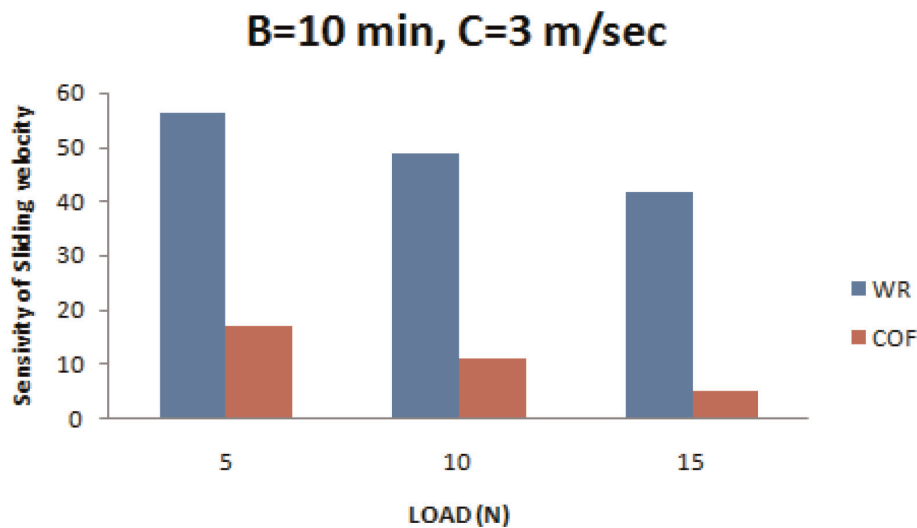


Figure 8.
Sensitivity analysis results of sliding velocity.

4.3 Sensitivity analysis

Figure 6 highlights the sensitivity analysis of load for WR and COF. Sensitivity analysis of load for WR and COF is negative for lower load values and it is negative as the value of sensitivity of load increases. **Figure 7** illustrates the time sensitivity. Time sensitivity for WR is positive for lower load values and it is positive as the value of sensitivity of load increases and COF remains unchanged. **Figure 8** reveals sliding velocity sensitivity. Sliding velocity sensitivity for WR is positive and increases with increase in load. COF is positive with increase in load.

5. Conclusions

- The developed regression prototypical is with success match the nearest predicted wear rate of cast AA 8011- 4% fly ash composites at 95% confidence level within the range of investigation.
- The wear rate of composite compound values strongly depends on the investigational limits, that is, normal load, time and sliding velocity.

- Wear rate increases as the sliding speed increases due to work hardening of the surface and crushing of the fly ash particles. The WR rises with the raise of the normal load. It is attributed to excessive damage to the composite. Wear rate increases dependably with regular interval due to deduction of the majority of the materials when exposed to sliding force.
- COF grows through an increase in sliding speed, whereas increase in coefficient of friction normal load decreases then before rises. The assessment of friction coefficient is raised nearly linear up to 10 minutes of impression and subsequently rests to constant.
- Response surface methodology has the potential for more stringent sensitivity analysis and may be used for optimal parameter estimation for other mathematical models.


IntechOpen

Author details

Subramaniam Magibalan
Department of Mechanical Engineering, K.S.R. College of Engineering,
Tiruchengode, Tamil Nadu, India

*Address all correspondence to: magibalan42@gmail.com

IntechOpen

© 2019 The Author(s). Licensee IntechOpen. This chapter is distributed under the terms of the Creative Commons Attribution License (<http://creativecommons.org/licenses/by/3.0>), which permits unrestricted use, distribution, and reproduction in any medium, provided the original work is properly cited. 

References

- [1] Suresh S, Moorthi NSV, Vettivel SC, Selvakumar N. Mechanical behavior and wear prediction of stir cast Al-TiB₂ composites using response surface methodology. *Materials & Design*. 2014; **59**:383
- [2] Radhika N, Raghu R. Dry sliding wear behaviour of aluminium Al-Si₁₂Cu/TiB₂ metal matrix composite using response surface methodology. *Tribology Letters*. 2015; **59**(1):2
- [3] Baradeswaran A, Vettivel SC, Perumal AE, Selvakumar N, Issac RF. Experimental investigation on mechanical behaviour, modelling and optimization of wear parameters of B₄C and graphite reinforced aluminium hybrid composites. *Materials & Design*. 2014; **63**:620
- [4] Koksall S, Ficici F, Kayikci R, Savas O. Experimental optimization of dry sliding wear behavior of in situ AlB₂/Al composite based on Taguchi's method. *Materials & Design*. 2012; **42**:124
- [5] Sahin Y. Wear behaviour of aluminium alloy and its composites reinforced by SiC particles using statistical analysis. *Materials & Design*. 2003; **24**(2):95
- [6] Al-qutub AM, Khalil A, Saheb N, Hakeem AS. Wear and friction behavior of Al6061 alloy reinforced with carbon nanotubes. *Wear*. 2013; **297**(1):752
- [7] Rao VR, Ramanaiah N, Sarcar MMM. Tribological properties of aluminium metal matrix composites (AA7075 reinforced with titanium carbide (TiC) particles). *International Journal of Advanced Science and Technology*. 2016; **88**:13
- [8] Baradeswaran A, Elayaperumal A. Effect of graphite on tribological and mechanical properties of AA7075 composites. *Tribology Transactions*. 2015; **58**(1):1
- [9] Mandal N, Roy H, Mondal B, Murmu NC, Mukhopadhyay SK. Mathematical modeling of wear characteristics of 6061 Al-alloy-SiCp composite using response surface methodology. *Journal of Materials Engineering and Performance*. 2012; **21**(1):17
- [10] Kumar BA, Murugan N, Dinaharan I. Dry sliding wear behavior of stir cast AA6061-T6/AlN p composite. *Transactions of Nonferrous Metals Society of China*. 2014; **24**(9): 2785
- [11] Dinaharan I, Murugan N. Dry sliding wear behavior of AA6061/ZrB₂ in-situ composite. *Transactions of Nonferrous Metals Society of China*. 2012; **22**(4):810
- [12] Selvi S, Rajasekar E. Theoretical and experimental investigation of wear characteristics of aluminum based metal matrix composites using RSM. *Journal of Mechanical Science and Technology*. 2015; **29**(2):785
- [13] Basavarajappa S, Chandramohan G. Dry sliding wear behavior of hybrid metal matrix composites. *Materials Science*. 2005; **11**(3):253
- [14] Rajmohan T, Palanikumar K, Ranganathan S. Evaluation of mechanical and wear properties of hybrid aluminium matrix composites. *Transactions of Nonferrous Metals Society of China*. 2013; **23**(9):2509
- [15] Senthilkumar C, Ganesan G. Electrical discharge surface coating of EN38 steel with WC/Ni composite electrode. *Journal of Advanced Microscopy Research*. 2015; **10**(3):202
- [16] Magibalan S, Senthilkumar P, Senthilkumar C, Palanivelu R, Prabu M. Dry sliding behavior of the aluminum alloy 8011 with 4% fly ash. *Materials Testing*. 2018; **60**(2):209

[17] Magibalan S, Senthilkumar P, Senthilkumar C, Palanivelu R, Prabu M. Dry sliding behavior of the aluminum alloy 8011 with 8% fly ash. *Materials Testing*. 2018;**60**(7-8):777

[18] Magibalan S, Senthilkumar P, Senthilkumar C, Palanivelu R, Shivasankaran N, Prabu M, et al. *Materials Research Express*. 2018;**5**(5): 056505

[19] Kim IS, Jeong YJ, Son IJ, Kim IJ, Kim JY, Kim IK, et al. Sensitivity analysis for process parameters influencing weld quality in robotic GMA welding process. *Journal of Materials Processing Technology*. 2003;**140**(1-3):676

[20] Palani PK, Murugan N. Sensitivity analysis for process parameters in cladding of stainless steel by flux cored arc welding, *Journal of Manufacturing Processes*. 2006;**8**(2):90

[21] Karaoğlu S, Seçgin. Sensitivity analysis of submerged arc welding process parameters. *Journal of Materials Processing Technology*. 2008;**202**(1-3): 500

[22] Lakshminarayanan AK, Balasubramanian V. Comparison of RSM with ANN in predicting tensile strength of friction stir welded AA7039 aluminium alloy joints. *Transactions of Nonferrous Metals Society of China*. 2009;**19**(1):9

[23] Straffelini G, Bonollo F, Molinari A, Tiziani A. Influence of matrix hardness on the dry sliding behaviour of 20 vol.% Al₂O₃-particulate-reinforced 6061 Al metal matrix composite, *Wear*. 1997;**211** (2):192

[24] Wang F, Liu H, Yang B. Effect of in-situ TiC particulate on the wear resistance of spray-deposited 7075 Al matrix composite. *Materials Characterization*. 2005;**54**(4-5):446